Mem. S.A.It. Suppl. Vol. 20, 84

Memorie della
Supplementi

Laboratory measurements of particulate samples of olivine and related planetological studies

F. Mancarella[1], A. Facchini[2], G. Liuzzi[1], A. Blanco[1], M. D'Elia[1], S. Fonti[1] and V. Orofino[1]

[1] Physics Department, University of Salento, Via Arnesano, 73100 Lecce (ITALY)
[2] IFSI, INAF, Area della Ricerca di TorVergata, Via del Fosso del Cavaliere 100, 00133 Roma (ITALY)
e-mail: francesca.mancarella@le.infn.it

Abstract In this work we present laboratory reflection measurements on olivine samples, analyzed in the wavelength range $0.2 \div 2.5\ \mu m$. Our purpose is to study the influence of the grain size on the spectra and in particular on the variations of the absorption feature at about $0.64\ \mu m$, whose reflectance peaks at $0.56\ \mu m$ and near $0.7\ \mu m$ have relative strengths, which are size dependent and well correlated. The identification of such feature in the observed spectra of Mars would provide useful information about the characteristics of the regolith present on the Martian surface; for this purpose, we analysed some reflectance spectra collected by the VIS-IR imaging spectrometer OMEGA on board of Mars Express.

Key words. Laboratory – spectroscopy – olivine – Mars – OMEGA

1. Introduction

Olivine ($(Mg, Fe)_2SiO_4$) is a rock-forming mineral, very abundant on planetary surfaces, consisting of an isomorphic mixture of forsterite (Mg_2SiO_4) and fayalite (Fe_2SiO_4). Its importance is due not only to its ubiquity in the Solar System, but also to the fact that, in presence of water, it readily alters to iddingsite and various phyllosilicates (Colman, 1986). For this reason, olivine plays an important role in the framework of the occurrence of surface water and geochemical evolution of celestial bodies.

Laboratory research on terrestrial particulate olivine samples allows to interpret the data coming from space missions. In the present work we show and discuss the experimental results concerning reflectance measurements in the $0.2 \div 2.5\ \mu m$ wavelength range, made on terrestrial particulate samples of olivine of different grain size; in the second part, we illustrate the comparison between laboratory results and Martian spectra, in order to obtain important information about the characteristics of the Martian regolith.

Send offprint requests to: F. Mancarella

2. Laboratory measurements

We produced several grain samples from three different kinds of olivine; one of these is the product of a grinding procedure started directly from a commercially available bulk sample collected in the German region of Eifel, while, the other two are produced starting from

some high purity gems (called Green Olivine and Forsterite, from Ward's Natural Science). These samples have been divided, using a set of sieves in six different size ranges:

(a) between 1000 and 425 μm;
(b) between 425 and 300 μm;
(c) between 300 and 200 μm;
(d) between 200 and 106 μm;
(e) between 106 and 50 μm;
(f) smaller than 50 μm.

The above size ranges, whose limiting values are imposed by the commercially available sieves, have been chosen in order to cover the whole size range of the Martian regolith (Jakosky et al., 2000).

The size distributions of the grains in the various size ranges have been evaluated by means of the granulometer Malvern Mastersizer 2000, which derives the dimensional information analysing the diffraction pattern of a laser beam. The result is a volume size distribution from which the effective diameter D of our samples in the six size ranges (Fig. 1) can be evaluated (Orofino et al., 2011).

For the reflectance measurements we used a Perkin Elmer Lambda 900 (PE-L900) spectrophotometer in the range $200 \div 2500$ nm equipped with a Labsphere integrating sphere in Spectralon of 150 mm. In Fig. 2 we report all the spectra relative to the six grain size fractions obtained for a sample of Green Olivine;

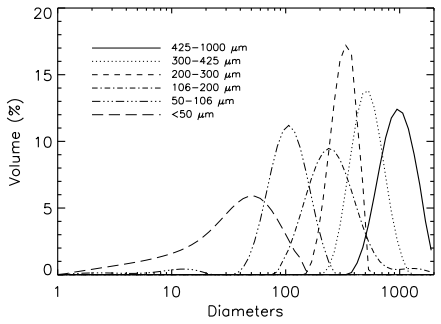

Fig. 1. Dimensional distributions of the Green Olivine samples.

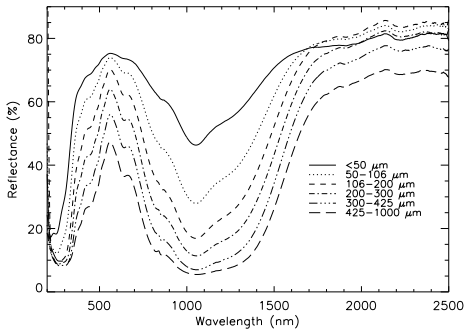

Fig. 2. Reflectance spectra of the Green Olivine samples in the selected size ranges.

similar spectra were collected for the other two kinds of olivine. As it can be seen in Fig. 2, the main feature present in all the spectra is that at about 1.0 μm due to the ferrous iron in olivine (Burns, 1970). Very interesting is also the band at 0.64 μm; the nature of this feature is still a matter of debate. Probably the most likely origin of this band is a spin-forbidden Fe^{2+} transition, as suggested by King and Ridley, (1987). However, in some samples of altered olivine (Orofino et al., 2006) it is likely that a fraction of the transitions originating the 0.64 μm band is also due to the Fe^{3+} ions. In other words, the band could be partially due to oxidized iron present in the olivine grains, as a results of their aqueous alteration.

This is not the case for the samples analyzed in this work. In fact, as shown in Fig. 3, the spectra of these olivines do not show the tipical bands, due to aqueous alteration, at 1.4, 1.9 and 2.3 μm (Clark et al., 1990). From Fig. 2 it is immediately evident that not only the continuum level increases and the spectral contrast decreases as the grain size becomes smaller but also the two reflectance maxima around the 0.64 μm absorption feature undergo evident changes both in position and in relative intensity. In detail, plotting the position of the two peaks against the average effective diameter D of the grains, the maxima shift towards shorter wavelengths as D increases (Orofino et al., 2006).

We also introduced a spectral parameter

$$\Delta_n(D) = \frac{R(\lambda_1) - R(\lambda_2)}{R(\lambda_1) + R(\lambda_2)} \quad (1)$$

where $R(\lambda_1)$ and $R(\lambda_2)$ are the measured reflectivity of the maxima at 0.56 μm and around 0.7 μm respectively. A common general trend exists for all the olivines we analyzed: Δ_n increases as D increases, although differences among the various types are not negligible.

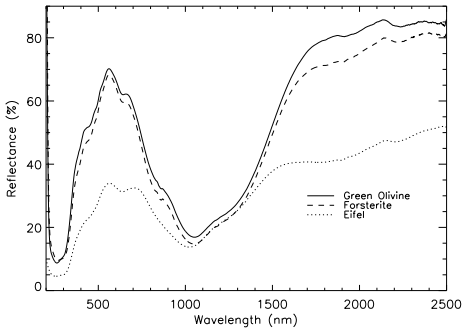

Fig. 3. Reflectance spectra of the three kinds of olivine analyzed in this work for the same granulometric class (106 – 200 μm).

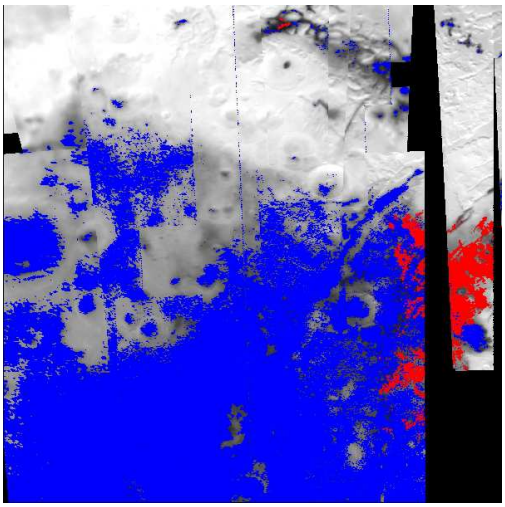

Fig. 4. Nili Fossae, part of Isidis Basin and Syrtis Major (15°−30°N, 65°−80°E). In red, pixels that are positive to the olivine spectral index, in blue, pixels that are positive to the pyroxenes spectral index, defined by Poulet et al., (2007)

3. OMEGA data analysis

Starting from the spectral behavior of olivine studied in laboratory, the analysis of the spectra collected by the spectrometer OMEGA (*Observatoire pour la Minéralogie, l'Eau, Les Glaces e l'Activité*, Bibring et al., 2005) was carried out with the aim to extract, from the surface spectra of Mars, the data concerning the visible bands, that is the 0.64 μm band and the relative 0.5 μm and 0.7 μm reflectance peaks. For this purpose, we analyzed two particular regions of Mars where olivine was identified by Koeppen and Hamilton, (2008): Nili Fossae, part of Isidis Basin and Syrtis Major (15°−30°N, 65°−80°E), and a portion of Valles Marineris around Aurorae Planum and Ganges Plasma (0° − 15°N, 45° − 60°W).

The analysis of OMEGA data in the visible channel does not require spectral and spatial co-registration between the visible and the infrared channel. On the other hand, in the visible spectral range it is difficult to identify bands with a weak spectral contrast such as olivine, because below 0.7 μm the spectrum of the martian surface presents a strong absorption band due to Fe^{3+} (Singer and McCord, 1979).

Each spatial pixel of the data mosaics covering the two martian regions that we have

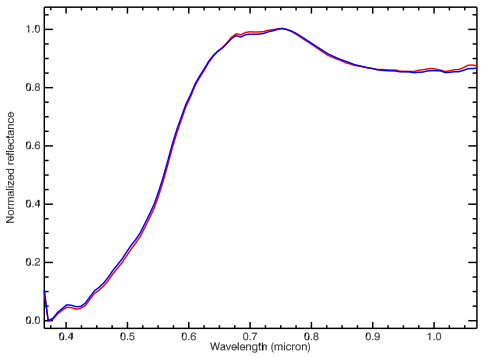

Fig. 5. Average spectra of olivine (red) and pyroxenes (blue) in Nili Fossae region.

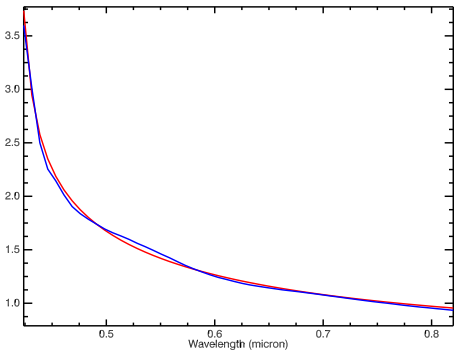

Fig. 6. In blue: ratio between average spectrum of pixels associated with the olivine index (red in Fig. 4) and an average spectrum without the 1 μm band (white in Fig. 4). In red: best-fit curve.

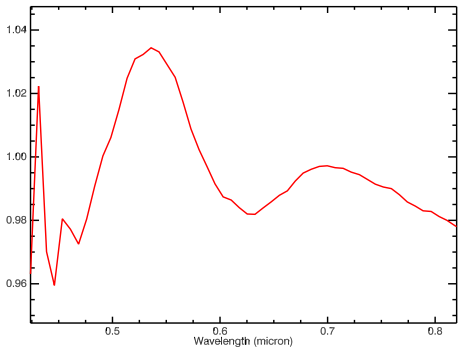

Fig. 7. Ratio between the two curves in Fig. 6. The visible olivine band around 0.64 μm and the relative peaks at 0.54 μm and 0.7 μm are visible.

studied contains a spectrum which varies according to the albedo of the surface; therefore, in order to compare areas with different albedo, as first step, we have normalized all spectra in the visible range ($0.36 \div 1.06\ \mu m$): for each spatial pixel, we required the reflectivity to be 0.0 at the wavelength related to the median of the minimum of all the spectra and 1.0 at the wavelength related to the median of the maximum of all the spectra. In Fig. 4, we show the spatial distribution on the mosaic data of the region of Nili Fossae in which we applied the spectral indexes defined by Poulet et al., (2007), related to olivine (in red) and pyroxenes (in blue), which are often associated in mixtures with olivine; while, in Fig. 5, we present the average normalized spectra refering to the previous spatial distributions (olivine and pyroxenes).

As it can be seen in Fig. 5, in the visible range, the average spectral behavior of olivine and pyroxenes is the same, so, in order to distinguish the visible bands of olivine we compared the average spectra of olivine and pyroxenes, obtained before, with a reference spectrum, namely the average spectrum of a region where the 1 μm band, typical both of olivine and pyroxenes, has a negligible spectral contrast. An analytic function (red curve in Fig. 6) has then been interpolated to the ratio between the spectra of minerals and the reference spectrum (blu curve in Fig. 6). In Fig. 7 is shown the ratio between the two curves in Fig. 6: it can been seen that the features are in the same wavelength position of the olivine bands in the visible range, obtained in laboratory. Furthermore we checked that the positions obtained with this method are independent of the choice of the analytic function; in fact, varying the function parameters in such a way that the chi-square was always acceptable, the intensities of the bands varied but not their wavelength positions.

The inability to determine the exact intensity of the peaks at 0.54 μm and 0.7 μm,

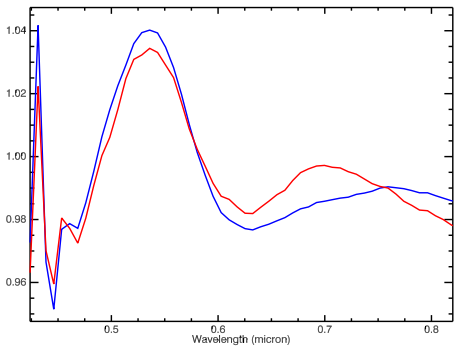

Fig. 8. Position of visible peaks of olivine (red) and pyroxenes (blue) in Nili Fossae.

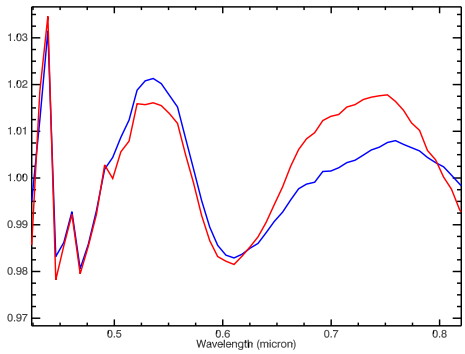

Fig. 9. Position of visible peaks of olivine (red) and pyroxenes (blue) in Valles Marineris.

which depends on the parameters of interpolated curve, makes it impossible to extract information about the granulometry of olivine on the martian surface. However, it is possible to evaluate the changes of the positions of the visible peaks in the case of different mixtures between olivine and pyroxenes.

The method, described before and tested on the average spectrum of olivine in Nili Fossae, was applied to the pyroxenes in the same region and to both minerals in Valles Marineris (Figs. 8 and 9).

Data analysis has been performed also to search for a possible correlation between the wavelength position of the maximum reflectance in the range $0.38 \div 1.06\ \mu m$ and the reflectance value at $0.68\ \mu m$ which corresponds to the beginning of the visible slope: Fig. 10 reports the 2D scatter plot of the spectra of Nili Fossae and in Fig. 11 the spatial distribution of the clusters identified in the previous scatter plot.

In Fig. 11 the cyan pixels identify a region where the spectral band at $1\ \mu m$ has a negligible spectral contrast: this distribution is in agreement with the spatial distribution of the pixels with a spectral index defined by Poulet et al., (2007) not related to olivine or pyroxenes (see Fig. 4). The green pixels are related to bad pixels introduced by instrumental errors and/or by an incorrect subtraction of the atmospheric contribution during data reduction. It is evident a correlation between the maximum in the range $0.38 \div 1.06\ \mu m$ and the reflectance value at $0.68\ \mu m$ for yellow and magenta pixels which are spatially distributed in the regions where Poulet et al., (2007) found olivine and pyroxenes in mixtures with different percentage or in mixtures with other minerals.

4. Conclusion and future developments

As already discussed in section 3, the method developed in this work is useful to determine the band positions of olivine and pyroxenes in the visible spectra of OMEGA data, but it is unable to give quantitative results on abundance of olivine in mixtures or on its grain size.

For a correct interpretation of the spectra obtained in Fig. 8 and 9, we need to analyze in laboratory samples of pyroxenes in order to study the behavior of these minerals in the visible range at various grain size and with different compositions. Firstly our analysis will focus on low calcium pyroxenes with different contents of iron. In a second step, we will study the spectroscopic behavior of olivine and pyroxenes mixtures with different percentages. We will continue our analysis of the OMEGA spectra applying our method to homogeneous data recorded in single orbits. In addition, we will verify the correlation found

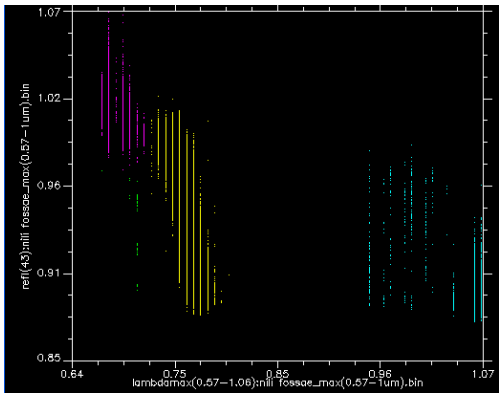

Fig. 10. 2D plot of pixels of Nili Fossae mosaic: reflectance at $0.68\ \mu m$ as a function of the wavelength position of the reflectance maximum.

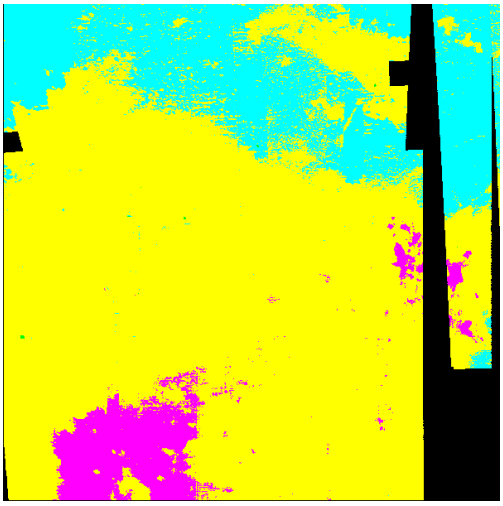

Fig. 11. Spatial distribution on Nili Fossae region of pixel clusters of Fig. 10 (see for comparison Fig. 4).

between the wavelength position of the maximum reflectance in the range $0.38 \div 1.06\ \mu m$ and the reflectance value at $0.68\ \mu m$ (Fig. 10) with a statistical approach using the cluster analysis..

Finally, we plan to extend our method to OMEGA data taken in various orbits related to different regions of martian surface and to regions observed with CRISM (*Compact Reconnaissance Imaging Spectrometer for Mars*) on board of Mars Reconnaissance Orbiter (Murchie et al., 2007).

References

Bibring, J.P. et al., 2005, Science, 307, 1576

Burns, R.G., 1970, Mineralogical Applications of Crystal Field Theory. Cambridge University Press, New York.

Clark, R.N. et al, 1990, J. Geophys. Res., 95, 12653

Colman, S.M., 1986. Rates of Chemical Weathering of Rocks and Minerals, Academic Press, Orlando, FL.

Jakosky, B.M. et al., 2000, J. Geophys. Res., 105, 9643

King, T.V.V. and Ridley, W.I., 1987, J. Geophys. Res., 92, 11457

Koeppen, W.C., & Hamilton, V.E., 2008, J. Geophys. Res., 113, E05001.

Murchie, S. et al.,2007, J. Geophys. Res.,112, E05S03.

Orofino, V. et al., 2006, Planet. Space. Sci., 54, 784

Orofino, V. et al., 2011, Mem.SAIt, suppl. 16, 113

Poulet, F. et al., 2007, J. Geophys. Res., 112, E08S02.

Singer, R.B., & McCord, T.B., 1979, Proc. Lunar Planet. Sci. Conf. 10th, 1835